Berenguer D. (Orcid ID: 0000-0001-9974-6475)

TGA/FTIR study of the pyrolysis of sodium citrate and its effect on the pyrolysis of tobacco and tobacco/SBA-15 mixtures under N_2 and air atmospheres.

A. Marcilla *, A. Gómez-Siurana, M. Beltrán, I. Martínez-Castellanos, I. Blasco and D. Berenguer

Dpto. Ingeniería Química, Universidad de Alicante, Apdo. 99, 03080 Alicante, Spain
Tel.: +34 96 590 2953; fax: +34 96 590 3826. *e-mail address: antonio.marcilla@ua.es

Abstract

In this work, the effect of sodium citrate mixed with tobacco, in presence and absence of SBA-15 material, was studied by TGA/FTIR under N_2 and air atmospheres. Depending on the atmosphere used, the decomposition of sodium citrate changes considerably at high temperatures, mainly due to the oxidation of the residue. The analysis of the experimental and calculated DTG data of the sodium citrate/SBA-15 mixtures allows the observation of marked widening of the peaks appearing at lower temperatures, due to the presence of SBA-15, while the expected peak at high temperatures in air completely disappears.

The presence of sodium citrate in tobacco and tobacco/SBA-15 mixtures produces changes, especially in air atmosphere, where the main peaks increase their intensity, whereas decreasing that of the oxidation of the residue at around 450 ºC and an important peak appears at 630 ºC. In N_2 atmosphere, all decomposition processes of tobacco proceed at lower temperatures and with higher intensities. The peak due to the citrate at temperatures around 200 ºC completely disappears in all samples.

Keyword

Sodium citrate, tobacco, SBA-15, FTIR

Introduction

In the European Union, tobacco cultivation covers about 100000 ha. Tobacco is grown in 12 countries of the European Union, being the main producers Italy, Bulgaria, Greece, Spain and Poland, which account for around 85% of the growing area. Moreover, the EU produces less than 3% of global yearly raw tobacco production, and imports some 400,000 tonnes per year, mainly from Africa and America[1].

Despite less than 1% of the world's total agricultural land is used for tobacco farming (Food and Agriculture Organisation of the United Nations)[2], the tobacco industry, cultivation, manufacture of tobacco products, and distribution and sale of products, taxes, affects favorably the economy of the countries. Moreover, smoking and its side effects cost the world's economies more than $1 trillion and kill more than 6 million people each year — with deaths expected to rise by more than a third by 2030, according to a new report from the World Health Organization and the National Cancer Institute[3]. Those losses exceed annual global revenue from tobacco taxes, estimated to be $269 billion in 2013-14. Of that, less than $1 billion was invested in tobacco control[3]. Consequently, researchs for reducing the toxicity of tobacco are great interested may have important effects on the global economy, both in the agriculture side as well on the public health side.

The manufacture of cigarettes involves the incorporation of up to 10 % (w/w) of tobacco additives that affect the smoking behavior and, in some cases, are intended to increase the

attractiveness of cigarettes. These compounds may influence taste, moisture, burn rate and smoke pH but also such sensory properties like harshness, smoothness and impact[4]. Potassium and sodium citrates are used as combustion modifiers, applied either to tobacco column paper or to tobacco itself. More than 600 substances are considered as tobacco additives[5-9], and it is known that many of these compounds may react to form different compounds during the pyrolysis and combustion processes involved in smoking cigarettes. Therefore, additives are increasingly subjected to analytical control, and tobacco legislation in several countries is under continuous development, posing severe restriction to many of them.

The European Parliament has empowered the European Commission to adopt further legislative acts to aid the implementation process of Directive 2014/40/EU[10] in order to reduce tobacco consumption among young people. This legislation takes the form of delegated or implementing acts that outline in more detail the rules and measures regarding tobacco and related products. They include the layout, design and shape of the combined health warnings for tobacco products for smoking, the position of the general warning and information message on roll-your-own tobacco in pouches, the reporting format for tobacco ingredients and emissions, define a priority list of additives which warrant further examination, and establish rules and mechanism for determining products with characterizing flavors. With respect to the additives, the new regulation bans flavors that increase the attractiveness of cigarettes and snuff rolling. For example, menthol in cigarettes will be prohibited from 2020[11]. In this way, the Commission shall establish a list of authorized additives in cigarettes and snuff rolling, and create a priority list of additives contained in cigarettes and roll-your-own tobacco subjected to enhanced reporting obligations. Nowadays, such priority list contains 15 substances, including cocoa, glycerol, sorbitol, and menthol among others[11].

Sodium and potassium citrates and phosphates are widely used as burn additives in cigarette papers because their ability to modify the rate of combustion. It has been reported that the thermal degradation of the cellulose structure starts at lower temperature in the presence of sodium citrate. Moreover, the width of paper burn line increases, and more oxygen is allowed to reach the coal for sustaining the smoldering combustion[12]. Sodium citrate has also been described as a flavor additive[5]. It is well known that alkaline metals naturally appearing in biomass have an influence on its thermal decomposition[13-18]. Potassium increases the rate of biomass pyrolysis as well as the gas and chars yields, and decreases the tar products. In the same way, it has been reported that sodium lowers the activation energy of biomass pyrolysis[19], and increases the percentage of ashes[20]. In general, the concentration of potassium in biomass is much higher than that of sodium, and perhaps this is the reason why potassium has been studied in more extent than sodium.

The use of zeolites and other aluminosilicates in the filter or directly mixed with tobacco in order to reduce nitrosamines and polycyclic aromatics in the tobacco mainstream smoke has been described by several authors[20-23], who checked the role of materials such NaA, NaY, KA and NaZSM-5, Cu-ZSM-5, SBA-15, MCM-48, Cerium-containing MCM-48, among others. The role of some of these materials on the pyrolysis and oxidation of tobacco as well as on different systems involving tobacco and different cigarette additives have been reported elsewhere[24-26].

Thermogravimetric analysis coupled to Fourier-transform infrared spectrometry (TGA-FTIR) has been revealed as a powerful tool for carrying out this type of studies[27,28] and has been widely applied for studying tobacco, tobacco additives and catalysts[25,28]. However, no TGA-FTIR

studies of the thermal decomposition of sodium citrate under air and N_2 atmospheres have been found in literature, and the effect of SBA-15 on these processes is also unknown, as well as the possible interactions among components appearing when mixtures of tobacco with both compounds are pyrolysed. In a previous work[29], the study by TGA-FTIR of the thermal decomposition of other citrate, potassium citrate, revealed that the process evolves in a similar way in N_2 and in air atmospheres below 320 ^{o}C, but differs in the last decomposition stages, and that the addition of SBA-15 seems to reduce the number of decomposition steps. SBA-15 was selected between a variety of materials due to its large pore size and its high total pore volume. Thus, the principal objective of the present work is to study by TGA/FTIR the effect of sodium citrate, when is mixed with tobacco, in the presence and in the absence of SBA-15, and in inert and oxidizing atmospheres, for obtaining a better insight on its decomposition processes and the effect of the SBA-15 material on such processes.

Experimental methods

Materials

SBA-15 catalyst (S) was synthesized according to the procedure described in the bibliography[24]. The textural characteristics of the SBA-15 were analysed by the corresponding N_2 adsorption isotherms at 77 K, measured in an automatic AUTOSORB-6 supplied by Quantachrome. The surface area, according to the BET method, was 757 m^2/g; the pore size distribution was obtained by applying the BJH model with cylindrical geometry of the pores, yielding an average pore diameter of 6.1 nm and a total pore volume of 1.06 cm^3/g.

Tobacco of the 3R4F cigarettes of the Reference Cigarette Program of the College of Agriculture of the University of Kentucky was used, and tri-sodium citrate di-hydrate of Alfa (Aesar) laboratories was supplied by VWR.

Tobacco samples were grinded and passed through a sieve of 20 microns in order to avoid the heterogeneity associated with the different tobacco fibres. Then, mixtures of tobacco (T) and 150 g Kg^{-1} of sodium citrate (C) (TC sample, according to the employed nomenclature), sample of tobacco with 150 g Kg^{-1} of SBA-15 (TS) and tobacco with 150 g Kg^{-1} of sodium citrate and 150 g Kg^{-1} of SBA-15 (sample TCS) were prepared. A mixture 1:1 of sodium citrate and SBA-15 (CS sample) was also prepared. To mix the components, sodium citrate was dissolved in the minimum necessary water, the obtained solution was added to tobacco, SBA-15 or tobacco SBA-15 mixture, and the samples were dried at 50 ^{o}C for 24 h. The samples which did not contain sodium citrate (T, TS, S) were prepared in a similar way, adding a small amount of water and dried under the same conditions.

TGA/FTIR Analysis

Samples T, TS, C, CS, TC and TCS were pyrolyzed under N_2 and air with a flow rate of 80 mL min^{-1} STP flow rate, in a TGA Metller Toledo thermobalance at a heating rate of 35 ^{o}C min^{-1}, from 25 ^{o}C up to 850 ^{o}C, with 20 min holding time at this temperature. The furnace of the thermobalance was connected to a Bruker Tensor 27 FTIR spectrometer through a heated line at 200 ^{o}C, in order to minimize the condensation of the less volatile compounds, thus allowing

the continuous FTIR analysis of the gases evolved at each temperature. Duplicate runs were carried out for all the samples.

Results

TGA analysis under N_2 atmosphere

Fig. 1 shows the weight loss curves (TGA curves) and the corresponding derivative curves (DTG curves) for the individual components of the mixtures studied: S, C and T. Table 1 shows the peak-temperatures corresponding to the DTG curves of all the samples studied. As can be seen, S presents a very simple trace and only shows a weight loss event, at low temperatures, corresponding to elimination of adsorbed moisture. C presents four decomposition steps; the first one, with DTG peak temperature around 168 ^{o}C and involving 12% of weight loss, corresponding to the elimination of water of crystallization[30,31]. The second stage, with maximum decomposition rate at 325 ^{o}C may be related to a partial degradation of sodium citrate, and the third stage, with DTG-peak temperature at 489 ^{o}C, is associated with the decomposition of the residues from the previous steps[32]. These steps are in good agreement with that described in the bibliography[24,34]. Moreover, an additional step of decomposition is observed at around 822 ^{o}C, which could be attributed to the formation of activated carbon, according to the mechanism suggested by Sevilla and Fuentes[32,33]. These authors reported that the pyrolysis of citrates and other organic salts of Na, K or Ca, at high temperatures (800 ^{o}C) and in N_2 atmosphere yields activated carbons, and suggested the following mechanism: firstly, at temperatures lower than 650 ^{o}C, the corresponding carbonate is formed. Such carbonate decomposes at higher temperatures to form the metal oxide and CO_2. After that,

the CO_2 evolved reacts with the carbonaceous residue to form CO, which generates microporosity. At the same time, the metal is produced via reduction of the corresponding oxide by carbon, playing a crucial role in the generation of additional porosity because their vapours are intercalated between the graphene layers, causing the swelling and disruption of the carbon microstructure.

Fig. 1 also shows the TGA and DTG curves corresponding to the pyrolysis of the reference tobacco, which has been already described in previous works[29], and involves, at least, the following six decomposition steps:

- Evaporation of moisture at temperatures lower than 130 °C;
- Evaporation of other volatile compounds in the range 160–220 °C;
- Two overlapped processes in the range 220–380 °C mainly corresponding to decomposition of hemicellulose (and other polymers) and cellulose, respectively;
- Pyrolysis of lignin in a wide range of temperature, with maximum reaction rate at around 480 °C;
- Dehydrogenation and aromatization of char at around 650 °C.

The considered mixtures (i.e., samples CS, TC, TS and TCS) were pyrolysed under the same conditions above described, and the experimental DTG traces have been compared with those obtained from the linear combination of the DTG of the single components, taking into account the mixture composition. We have named such traces as "theoretical", and they have been identified by adding a “t” after the corresponding mixture name. Table 2 shows the

experimental final residues obtained for all the samples together to the expected theoretical values. The differences among samples, as well as the effect of the different additives used, are more clearly seen when comparing each curve with its corresponding theoretical curve. Fig 2 shows the results of this comparison for the four mixtures studied. As can be seen, the pyrolysis of C (Fig. 2a) is noticeably affected by the presence of S material, which advances and widens the main decomposition steps: the three DTG peaks are displaced from 168 ^{o}C, 325 ^{o}C and 489 ^{o}C in the absence of SBA-15, towards 72 ^{o}C, 297 ^{o}C and 453 ^{o}C, respectively when mixed with that compound. Moreover, the final step related to the porous carbons formation completely disappears in the presence of the catalyst. According to Table 2, the final residue observed (683 g Kg-^{1}) is lower than expected (766 g Kg-^{1}), suggesting that the S material increases the weight loss involved in the decomposition of C and yields a very stable residue which does not react further.

Fig. 2b shows the experimental and theoretical DTG traces for the mixture TC. The noticeable interaction between tobacco and citrate can be observed, resulting in three main effects. The first one is related to the apparent disappearance of the citrate dehydration process step (i.e., the expected peak at around 168 ^{o}C), suggesting that the crystallization of sodium citrate, once mixed with tobacco as described in the "Experimental methods" section, proceeds in a different way as pure sodium citrate, and avoids the presence of hydration water inside crystals. The result is a very wide peak appearing at intermediate temperatures between those corresponding to the loss of moisture and loss of hydration water in the sample without catalyst. The second effect consists in a displacement of the main decomposition steps of tobacco towards lower temperatures. Finally, the presence the Na cation, that at these temperatures is found in its oxide form[32,33], provokes an unexpected process appearing at high

temperatures (between 610-825 ^{o}C), resulting in a decrease of the final residue in comparison with the expected value (according to Table 2, 256 g Kg-^{1} versus 374 g Kg-^{1}), thus suggesting that sodium citrate significantly alters not only the temperatures of the different decomposition steps but the yields and the chemical nature of the different compounds involved. Similar tendency was observed by Gao et al.[34], who analyzed by TGA samples of reconstituted tobacco with sodium citrate. These authors identified a weight loss peak corresponding to the elimination of water and other volatiles, two sharp weight loss peaks associated with the decomposition of hemicellulose and cellulose and elimination of lignin, another weight loss related to the thermal oxidative decomposition of char. Finally, at temperatures higher than 600 °C, Gao et al. reported a small DTG-peak at about 650 °C associated with the thermal decomposition of $CaCO_3$ and other salts.

Fig. 2c shows the comparison between the experimental and theoretical DTG curves of TS mixture. The effect of the catalyst has been described elsewhere[25], and can be summarised as a decrease of the intensity of the main decomposition processes, and an increase of the first one and those occurring at temperatures above 400 ^{o}C. As can be seen, a decrease of the intensity of the DTG-peaks at around 189 ^{o}C, 268 ^{o}C and 319 ^{o}C, and an increase of that below 100 ^{o}C and 447 ^{o}C occur, perhaps related to the different amounts of materials decomposing at each step or to the different composition of the gases evolved. In good agreement with the higher amount of final residue obtained from TS sample in comparison with the expected theoretical value (336 g Kg-^{1} and 291 g Kg-^{1}, respectively, according to Table 2), is the final decomposition step observed in the TS curve and may be related to the known effect of this type of catalysts promoting coke formation.

Finally, Fig. 2d shows the experimental and calculated curves corresponding to the ternary TCS mixture. In this case, the effects of C and S on T (the main compound) compensate each other, resulting one closer theoretical and experimental curve.

TGA analysis under air atmosphere

Fig. 3 shows the TGA and DTG curves corresponding to the thermal degradation of S, C and T under air atmosphere. The temperatures corresponding to the DTG peaks and the amount of residue obtained are shown in Tables 1 and 2, respectively. As expected, the behaviour of S is very similar to that observed in inert atmosphere (Fig. 1), showing only a water loss step at low temperatures. The decomposition of sodium citrate in air atmosphere is also very similar to that in N_2, at temperatures below 500 ºC (Fig. 3 and 1, respectively) and the DTG-peaks corresponding to the dehydration occurs at 168 ^{o}C, the partial degradation at 326 ^{o}C, and residue decomposition at 483 ^{o}C. Nevertheless, in air atmosphere, another process takes place (DTG-peak at 525ºC) and the last process, at 809 ^{o}C, sharpens markedly in this atmosphere, thus suggesting that oxygen enhances the above-mentioned gasification of the carbonaceous residue step.

The thermal degradation of tobacco in air atmosphere has been discussed elsewhere[25] and, as can be seen in Fig. 3, presents a moisture loss step (peak at 99 ^{o}C), a second decomposition step due to the evaporation of volatiles (at 182 ^{o}C), two overlapped processes in the range 220–380 °C mainly corresponding to the decomposition of hemicellulose and cellulose, respectively. The peaks observed in the range of 380-530 ^{o}C are the result of overlapped oxidation and pyrolysis processes, whereas the DTG-peak at around 656 ^{o}C must be related to

dehydrogenation and aromatization of the char and decomposition of endogenous inorganic compounds as carbonates.

According to Fig. 4a, the differences observed between experimental and calculated (as previously described) curves suggest noticeable changes in the pyrolytic behavior of sodium citrate because of the presence of the catalyst, being this changes more marked than those occurring in inert atmosphere (Fig. 2a). The DTG-peak obtained at around 167 ^{o}C in the absence of S, corresponding to the dehydration process, is shifted towards lower temperatures, as in nitrogen atmosphere (Fig. 2a), and its intensity increases markedly. On the other hand, the peaks at 483 ^{o}C and 525 ^{o}C appear now as a very small peak, almost a shoulder of the main peak, at 412 ^{o}C. As was observed in nitrogen atmosphere, the final residue obtained is very stable, and the amount is lower than the expected one (Table 2). The case of the TC mixture has been represented in Fig. 4b. As can be seen, the addition of sodium citrate produces noticeable changes in the thermal degradation of tobacco in air atmosphere. The peak corresponding to the dehydration of sodium citrate disappears when mixed with tobacco; the first peaks of tobacco decomposition are somewhat advanced and the intensity of the second one markedly increases; moreover, the main tobacco oxidation peak almost disappears in the presence of sodium citrate and a new fast sharp process appear at around 630 ºC. The amount of final residue obtained from TC sample (Table 2) is some lower than that expected, showing that sodium citrate also enhances the last decomposition steps of tobacco. Fig. 4c shows the experimental and calculated DTG-curves corresponding to the TS sample. The effect of S on the DTG curve of 3R4F tobacco decomposition in oxidizing atmosphere is somewhat similar to that observed in the presence of MCM-41[25], and mainly results in an increase of the intensity of the peaks at around 182 ^{o}C and 427 ^{o}C, and a decrease of those at

temperatures below 100 °C and around 325 °C. The final residue is also slightly lower than expected (Table 2). Finally, Fig. 4d shows the experimental and calculated curves corresponding to TCS sample, showing that in this case, the combined above-described effect of both compounds is observed. Effectively, the behavior at temperatures below 400 °C is somewhat similar to that observed in the case of the TC sample (despite SBA-15 also increased the intensity of the main DTG-peak in this range of temperature). Nevertheless, the shape of the experimental DTG-curve at temperatures above 400 °C seems to be a combination between those corresponding to TC and TS samples (Fig. 4b and 4c, respectively). As in the previous cases, the residue is somewhat lower than expected (Table 2). These features can be explained considering that, at high temperatures and in the presence of SBA-15 and oxygen, the effect of the sodium citrate remaining residue is not the same than when no catalyst was present.

FTIR analysis under N_2 and air atmospheres

In order to get a better insight on the thermal processes undergone by the samples, the gases evolved from the different decomposition stages have been studied by TGA/FTIR. Typically, the results can be analyzed from three points of view: i.e.: the 3D plots of intensity vs time (or temperature) and wavenumber, the evolution with temperature of the whole IR spectrum or the evolution with temperature of selected absorption bands. In the present paper we have selected the latter two.

In order to obtain a qualitative idea of the composition of the gases evolved at each decomposition step, the FTIR spectra corresponding to the gases arriving to the FTIR cell at the temperatures corresponding to several significant DTG-peaks have been extracted and the absorption bands assigned. In good agreement with the interpretation of the respective decomposition steps, the FTIR spectrum of de gases evolved from sodium citrate pyrolysis in inert atmosphere indicates that the signal of the gases evolved at 168 ^{o}C (Fig 5) corresponds to water, with the characteristic bands in the range of 4000–3500 cm^{-1} and 1800–1300 cm^{-1}. Practically, the only compound observed at 325 ^{o}C is CO_2 (bands at 2322 and 2355 cm^{-1}), as a consequence of the decarboxylation of the salt. At around 489 ^{o} C, besides CO_2, intense bands of carbonyl groups (1800–1710 cm^{-1}), and typical bands of alcohols and other hydroxyl compounds appear (C-O bonds in the range of 1145–1210 cm^{-1}, C-H bonds at around 3018 cm^{-1} and O-H bonds at 1313 cm^{-1}). At 822 ^{o}C (Fig 5) the spectrum is dominated by CO_2, though clear carbon monoxide bands, in the range 2190 and 2120 cm^{-1}, are also present, as a consequence of the gasification of the residue by carbon dioxide[34,35].

The spectra of the gases evolved from the pyrolysis of tobacco in N_2 atmosphere have been described elsewhere[29] and also agree with those presented in Fig. 6. On the other hand, the results obtained in air atmosphere for C and T (Fig. 7 and 8, respectively) only differ noticeably from those in inert atmosphere at temperatures higher than 400 ^{o}C, where the importance of the oxidation or combustion processes increases in a significant way. Thus, as expected, in air atmosphere, the gases evolved from sodium citrate at 483 ^{o}C (Fig. 7) contain much less oxygenated compounds, and at temperatures higher than 800 ^{o}C the yield of CO decreases almost disappearing. In both cases, this decrease occurs at expenses of CO_2, as a consequence of more complete oxidation reactions in the presence of O_2. The case of tobacco (Fig. 8) is also

similar, and the main component of the gases evolved at temperatures higher than 400 ^{o}C is CO_2.

The analysis of the evolution of the several selected IR bands provides complementary information. We have analyzed these data and compared to those obtained as the linear combination of those corresponding to the components of the mixture, in a way similar to that described for the DTG signals. We have grouped the figures corresponding to each wavenumber selected and each sample in both atmospheres. The different IR bands selected as characteristic of the gases evolved in the pyrolysis of tobacco and citrate are: CO_2 band at 2355 cm^{-1}, CO band at 2190 cm^{-1}, carbonyl band at 1749 cm^{-1}, water band at 3565 cm^{-1}, methylene band at 2830 cm^{-1}, and methane band at 3015 cm^{-1}.

CO_2 is the main signal in all cases, and its evolution with temperature is roughly similar to the DTG signal. The commented effects of the catalyst on the sodium citrate and tobacco samples are evident from this signal (see Fig. 9). Carbon monoxide follows a different pattern (Fig. 9b). When sodium citrate is being decomposed in presence of the catalyst, CO increases markedly during the decomposition step at around (440 ^{o}C), whereas it disappears during the last step, proving that the catalyst avoids the last oxidation of the residue obtained when no catalyst was present. Thus, indicate that the nature of such residues is completely different. Samples containing tobacco present the same processes expected, tough the intensity is somewhat higher than expected.

The carbonyl band (Fig. 9c) shows that when the salt is decomposed in the presence of the catalyst the main peak is highly reduced. In the case of tobacco with catalyst, only a slight increase is observed at temperatures above the main peak. Samples with tobacco and sodium

citrate and tobacco with sodium citrate and catalyst show that both, the tobacco and the catalyst produce a strong modification of the decomposition of the sodium citrate, since the expected peak at temperatures around 472 ^{o}C and corresponding to the salt are not present.

Water bands (Fig. 9d) show the already commented on behavior in the case of the dehydration of the salt, and the expected peak is strongly modified. Samples including tobacco and citrate present an increase of water evolution during the main decomposition peak.

Methylene bands (Fig. 9e) at around 458 ^{o}C are much lower than expected when decomposing sodium citrate in presence of the catalyst. Slight modifications in intensity are observed in the case of tobacco with catalyst (somewhat lower than expected) and in the case of tobacco and citrate (somewhat higher). When the two additives are present, both effects are compensated. Methane shows a similar behavior to methylene (Fig. 9f).

Sodium citrate in the presence of SBA-15 (CS) presents a single sharp intense peak at around 275 ^{o}C and a small shoulder. The other processes expected have completely disappeared showing the strong interaction of the SBA-15 on the oxidative degradation of sodium citrate.

In the presence of oxygen, as show in the TG, the effects are more marked. Fig. 10a shows the evolution of the CO_2 band with temperature. In the case of the sodium citrate and SBA-15 the behavior is completely similar to the DTG curve (Fig. 4a) except for the peak observed in DTG at low temperature that correspond to water elimination. In comparison with DTG of C, the addition of S material (CS) provokes the disappearance of the peak at 822 ^{o}C associated with the elimination of CO_2 (Fig. 7). This is another prove of the different nature of the residue

obtained under these conditions that cannot undergone the final oxidation step. Tobacco sample with catalyst shows an increase of the intensity of the CO_2 peak at low temperature. The main differences are observed in the samples with tobacco and citrate and tobacco and citrate and catalyst. In the first case, the second peak (the main expected) is strongly reduced, and a third very intense peak at high temperatures, appears similarly to that show in Fig. 4b and 4d.

CO evolution from sodium citrate with catalyst in air atmosphere shows a marked increase and a displacement to low temperatures (Fig. 10b). Tobacco sample with catalyst show a slight increase of the first peak. Tobacco citrate sample shows marked decrease of the peak at around 440 ^{o}C. A third peak appears at temperatures around 630 ^{o}C. The sample of tobacco and sodium citrate and catalyst shows and increase in the intensity of the first peak and a decrease of that of the second expected peak.

Carbonyl band (Fig. 10c) shows strong modifications in the case of sodium citrate in the presence of SBA-15, and a large peak is observed at around 300 ^{o}C. The rest of the samples behave similarly to those described when using nitrogen atmosphere.

Water (Fig. 10d) presents a similar behavior as that describe in the case of nitrogen atmosphere for the sample corresponding to sodium citrate with catalyst. The behavior in the case of tobacco with catalyst is very close to that expected, and only a slight increase in the peak at around 30 ^{o}C is observed. Nevertheless, in the case of tobacco with citrate and tobacco with citrate and catalyst, the main peak expected is much reduced, and another peak appears at higher temperatures, thus proving a strong interaction in these systems.

In air atmosphere, the bands of methylene and methane were not detected by FTIR.

Conclusions

The pyrolysis of sodium citrate, tobacco and SBA-15 as well as their binary and ternary mixtures have been studied by TG/FTIR under N_2 and air atmospheres up to 850 ^{o}C. The TG data as well as the IR representative bands has been analyzed by comparing the experimental results with those calculated as the linear combination of those of the single components of the samples. This procedure clearly reveals the existence of some interaction among the different compounds as well as its effect on the behavior of the mixed samples.

Citrate decomposes through four main processes under both atmospheres. The first decomposition step corresponds to the loss of crystallization water. Decomposition at temperatures below 400 ^{o}C occur in a similar way regardless the atmosphere. Nevertheless, oxidizing atmosphere involves changes at high temperatures, where an additional oxidation process takes place in the range of 425-550 ^{o}C, and sharpens the final oxidation process of the residue at temperatures above 800 ^{o}C. The addition of SBA-15 produces marked changes in the decomposition of sodium citrate, advancing all the observed processes, and hindering the final step of gasification of the residue.

The addition of SBA-15 practically does not change the temperature of the decomposition of tobacco in both atmospheres. Moreover, decreases the intensity of the decomposition steps observed in TG (in N_2 and air atmospheres), with the only exception of the stage related to the elimination of lignin in N_2 atmosphere. The pyrolytic behavior of tobacco changes in the presence of sodium citrate, mainly under air atmospheres. The presence of the organic salt

provokes a decrease of the temperature at which the decomposition processes occurs, and increases their intensity, with the only exception of the main oxidation process observed when no sodium citrate was added, that has almost disappeared. In the sample with tobacco, citrate and SBA-15, it is observed is an intermediate behavior between citrate and SBA-15 in both atmospheres.

In N_2 atmosphere, carbonyl compounds and CO_2 seem to be mainly formed at the lower decomposition temperature of tobacco, whereas at higher temperatures, an increase in the yields of CO, methane and methyl groups is observed in the gases evolved from the pyrolysis of TS, TC and TCS samples. As expected, for all the studied systems, the yields of CO_2 increase noticeably under air atmosphere. The differences found between the experimental and theoretical curves corresponding to the evolution with the temperature of the selected IR bands from the TC sample suggest the existence of an important interaction between citrate and tobacco. This effect is especially noticeable in the case of CO_2 and CO bands, thus, it could be concluded that sodium citrate modifies the mechanism of formation of these compounds during the decomposition of tobacco.

Acknowledgements

Financial support for this investigation has been provided by the Spanish Ministerio de Economía, Industria y Competitividad (CTQ2015-70726/P), and the Generalitat Valenciana (PROMETEO2016/056).

References

1. European Commission, https://ec.europa.eu/agriculture/tobacco_es

2. Food and Agriculture Organisation of the United Nations http://www.fao.org/home/en/

3. U.S. National Cancer Institute and World Health Organization. The Economics of Tobacco and Tobacco Control. National Cancer Institute Tobacco Control Monograph 21. NIH Publication No. 16-CA-8029A. Bethesda, MD: U.S. (2016).

4. Wayne GF, Chemical Additives in Cigarettes**,** Document prepared for WHO Scientific Advisory Committee on Tobacco Product Regulation, (2002).

5. Baker RR, Pereira da Silva JR, Smith G, The effect of tobacco ingredients on smoke chemistry. Part I: Flavourings and additives, Food Chem Toxicol. 2004; S3-S37: 42.

6. Gaworski CL, Dozier MM, Heck JD, Gerhart JM, Rajendran N, David RM, Brennecke L., Morrissey R, Toxicologic evaluation of flavor ingredients added to cigarette tobacco: 13-week inhalation exposures in rats, Inhal Toxicol. 1997;10: 357-381

7. Philip Morris LTD., Australia Ingredients Report—Composite List of Tobacco Ingredients, Reporting Period December 2000 to March 2001, Pursuant to Clause 6.3 (ii) of the Agreement between Commonwealth and the Manufacturers, (2000)

8. British American Tobacco Australia, Australia ingredients report, Composite List of Tobacco Ingredients, Reporting Period December 2000 to March 2001, Pursuant to Clause 6.3 (i) of the Agreement between Commonwealth and the Manufacturers, (2001)

9. Department of Health London, Permitted Additives to Tabacco Products in the United Kingdom, (2000)

10. European Commission

http://ec.europa.eu/health/tobacco/products/revision/implementation_en

11. European Union law, EUR-Lex Access to European Union law http://eur-lex.europa.eu/legal-content/EN/TXT/?uri=uriserv:OJ.L_.2016.131.01.0088.01.ENG&toc=OJ:L:2016:131:TOC

12. Krasny JF, Cigarette Ignition of Soft Furnishings, Technical Study Group Cigarette Safety Act of 1984, (1987)

13. Dayton DC, French RJ, Milne TA, Direct observation of alkali vapor release during biomass combustion and gasification. 1. Application of molecular beam/mass spectrometry to switchgrass combustion, Energy Fuels. 1995; 9(5): 855–865.

14. Darvell LI, Jones JM, Nowakowski DJ, Pourkashanian M, Williams A, Impact of minerals and alkali metals on willow combustion properties, World Renewable Energy Congress. 20005, p. 584-589

15. Fuentes ME, Nowakowski DJ, Kubacki ML, Cove JM, Bridgeman TG, Jones JM, Survey of influence of biomass mineral matter in thermochemical conversion of short rotation willow coppice, J Energy Inst. 2008; 81: 234–241.

16. Nowakowski DJ, Jones JM, Brydson RMD, Ross AB, Potassium catalysis in the pyrolysis behaviour of short rotation willow coppice, Fuel 20007; 86(15): 2389–2402

17. Fu Q, Argyropoulos DS, Tilotta DC, Lucia LA, Understanding the pyrolysis of CCA-treated wood: part I. Effect of metal ions, J Anal Appl Pyrolysis. 2008; 81(1): 60–64.

18. Williams PT, Horne PA, The role of metal salts in the pyrolysis of biomass, Rene. Energ. 1994; 4(1): 1–13.

19. Philpot CW, Influence of mineral content on the pyrolysis of plant materials, Forest Sci. 1970; 16: 461–471.

20. Cvetkovic N, Adnadjevich B, Nikolic M, Catalytic reduction of NO and NO_x content in tobacco smoke, Beitr. Tabakforsch. Int. 2002; 2: 43–48.

21. Xu Y, Zhu JH, Ma LL, Ji A, Wei YL, Shang X, Removing nitrosamines from mainstream smoke of cigarettes by zeolites, Micropor. Mesopor. Mater. 2003; 60: 125–138.

22. Yong G, Jin Z, Tong H, Yan X, Li G, Liu S, Selective reduction of bulky polycyclic aromatic hydrocarbons from mainstream smoke of cigarettes by mesoporous materials Micropor. Mesopor. Mater. 2006; 91: 238–243.

23. Marcilla A, Beltrán M, Gómez A, Navarro R, Berenguer D, Martínez I, Tobacco-catalyst mixtures for reducing the toxic compounds present in tobacco smoke. EURO-PCT078230349, Spain, (2009)

24. Gómez-Siurana A, Marcilla A, Beltrán M, Berenguer D, Martínez-Castellanos I, Catalá L, Menargues S, TGA/FTIR study of the MCM-41-catalytic pyrolysis of tobacco and tobacco–glycerol mixtures, Thermochim Acta. 2014; 587: 24–32.

25. Gómez-Siurana A, Marcilla A, Beltran M, Martinez I, Berenguer D, García-Martínez R, Hernández-Selva T, Study of the oxidative pyrolysis of tobacco–sorbitol–saccharose mixtures in the presence of MCM-41, Thermochim Acta. 2012; 530: 87–94.

26. Baker RR, Coburn S, Liu C, Tetteh J, Pyrolysis of saccharide tobacco ingredients: a TGA-FTIR investigation, J Anal Appl Pyrolysis. 2005; 74: 171–180.

27. Wang W, Wang Y, Yang L, Liu B, lan M, Sun W, Studies on thermal behavior of reconstituted tobacco sheet, Thermochim Acta. 2005; 437: 7–11

28. Gómez-Siurana A, Marcilla A, Beltrán M, Berenguer D, Martínez-Castellanos I, Menargues S, TGA/FTIR study of tobacco and glycerol-tobacco mixtures, Thermochim Acta. 2013; 573: 146-157.

29. Marcilla A, Gómez A, Beltrán M, Berenguer D, Martínez I and Blasco I, TGA-FTIR study of the thermal and SBA-15-catalytic pyrolysis of potassium citrate under nitrogen and air atmospheres, J Anal Appl Pyrolysis. 2017; 125: 144-152.

30. Bai H, Yanga L, Zhang J, Li L, Hua C, Lva J, Guoa Y, High-efficiency carbon-supported platinum catalysts stabilized with sodium citrate for methanol oxidation, J Power Sour. 2010; 195: 2653–2658.

31. Gao J, Wang Y, Hao H, Investigations on dehydration processes of trisodium citrate hydrates, Front Chem Sci Eng. 2012; 6(3): 276–281.

32. Sevilla M and Fuertes AB, A general and facile synthesis strategy towards highly porous carbons: carbonization of organic salts, J Mater Chem A. 2013; 1: 13738-13741.

33. Sevilla M. and Fuertes AB, Direct Synthesis of Highly Porous Interconnected Carbon Nanosheets and Their Application as High Performance Supercapacitors, J Am Chem Soc. 2014; 8(5): 5069–5078.

34. Gao W, Chen K, Yang R, Yang F, Process for coating of reconstituted tobacco sheet with citrates, J Anal Appl Pyrolysis. 2015; 114: 138–142.

35. Marcilla A, Beltran MI, Gómez-Siurana A, Martinez-Castellanos I, Berenguer D, Pastor V, García AN, TGA/FTIR Study of the Pyrolysis of Diammonium Hydrogen Phosphate-Tobacco Mixtures, J Anal Appl Pyrolysis. 2015; 112: 48-55.

TABLE CAPTION

Table 1. Temperatures of maximum decomposition rate (^{o}C) of the different decomposition steps for the studied systems in N_2 and air atmosphere.

Table 2. Experimental and calculated percentage of final residue (w/w %) obtained at 850 ^{o}C and after 20 min at 850 ^{o}C.

FIGURE CAPTION

Figure 1. TGA and DTG curves in N_2 atmosphere for the pyrolysis of S, C and T.

Figure 2. Experimental and theoretical DTG curves corresponding to the pyrolysis : a) C, b) TC, c) TS and d) TCS and sample in N_2 atmosphere..

Figure 3. TGA and DTG curves under Air atmosphere for the pyrolysis of S, C and T.

Figure 4. Experimental and theoretical DTG curves corresponding to the pyrolysis of: a) C, b) TC, c) TS and d) TCS and sample in air atmosphere.

Figure 5. FTIR spectra corresponding to the gas evolved at several selected temperatures in the TGA analysis in N_2 atmosphere of sodium citrate: a) 168 ºC, b) 325ºC, c) 489 ºC and d) 822 ºC.

Figure 6. FTIR spectra corresponding to the gas evolved at several selected temperatures in the TGA analysis in N_2 atmosphere of tobacco: a) 98 ºC, b) 182 ºC, c) 268 ºC, d) 319 ºC, e) 440 ºC and f) 686 ºC.

Figure 7. FTIR spectra corresponding to the gas evolved at several selected temperatures in the TGA analysis in Air atmosphere of sodium citrate: a) 168 ºC, b) 326 ºC, c) 483 ºC, d) 525 ºC and e) 809 ºC

Figure 8. FTIR spectra corresponding to the gas evolved at several selected temperatures in the TGA analysis in Air atmosphere tobacco: a) 98 ºC, b) 182 ºC, c) 269 ºC, d) 314 ºC, e) 427 ºC, f) 481 ºC and g) 656 ºC.

Figure 9. Comparison of experimental and theoretical curves of the evolution with temperature in N_2 atmosphere of: a) CO_2 band, b) CO band, c) carbonyl band, e) H_2O band, f) $-CH_3$ band, e) methane band.

Figure 10. Comparison of experimental and theoretical curves of the evolution with temperature in Air atmosphere of: a) CO_2 band, b) CO band, c) carbonyl band and e) H_2O band.

Table 1. Temperatures of maximum decomposition rate (ºC) of the different decomposition steps for the studied systems in N_2 and air atmosphere.

	System	Step 1	Step 2	Step 3	Step 4	Step 5	Step 6	Step 7
	C	168	325	489	822			
	CS	72	297	453				
N_2	**T**	99	182	268	319	(360-580) 439	686	
	TS	72	189	268	319	(360-550) 447	683	823
	TC	99	16	261	304	(350-550) 432	(610-825) 734	
	TCS	78	182	261	304	(360-550) 432	686	
	C	168	326	483	525	809		
	CS	72	319	412				
Air	**T**	99	182	269	314	427	481	(560-725) 656
	TS	79	189	269	314	442	473	(570-675) 656
	TC	98	168	262	292	448	519	630
	TCS	79	182	262	299	435	464	588

Table 2. Experimental and calculated percentage of final residue (w/w %) obtained at 850 ºC and after 20 min at 850 ºC.

		At 850 ºC		After 20 min 850ºC	
	System	**Experimental residue ($g\ Kg^{-1}$)**	**Theoretical residue ($g\ Kg^{-1}$)**	**Experimental residue ($g\ Kg^{-1}$)**	**Theoretical residue ($g\ Kg^{-1}$)**
N_2	**C**	588	588	471	471
	CS	683	766	675	704
	T	241	241	151	151
	TS	336	291	246	271
	TC	256	374	90	191
	TCS	335	348	219	291
Air	**C**	518	518	450	450
	CS	652	722	645	688
	T	111	111	94	94
	TS	158	170	198	221
	TC	230	265	125	146
	TCS	201	235	222	244

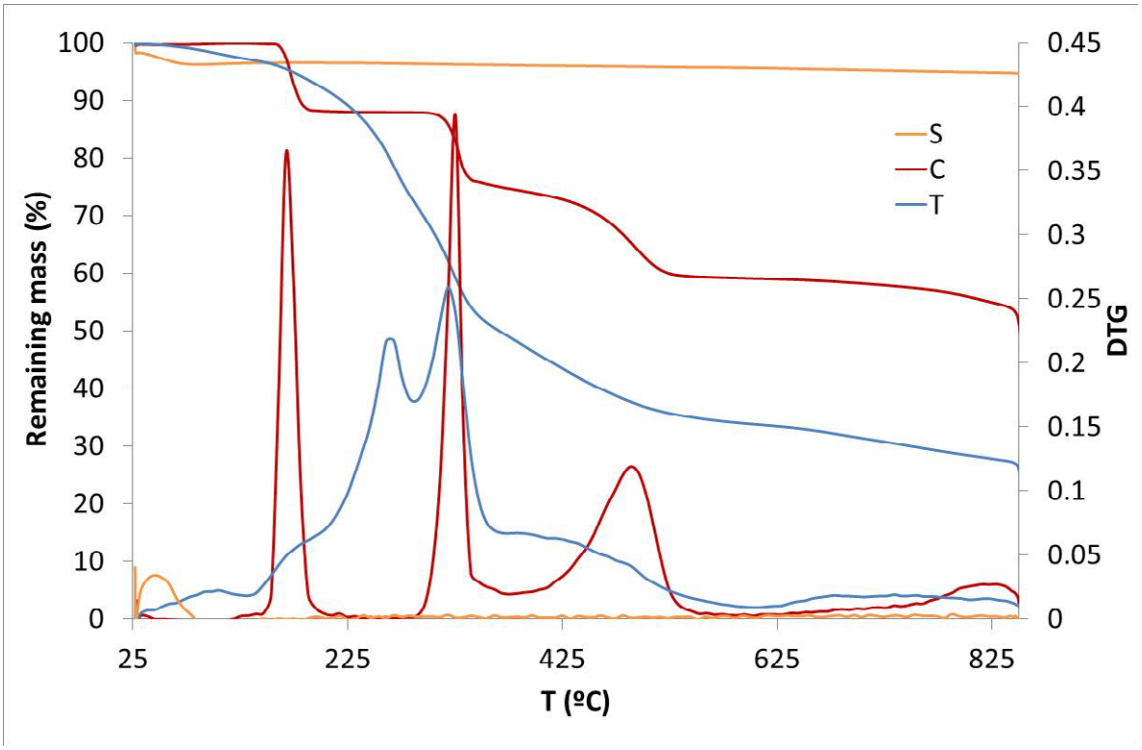

Figure 1. TGA and DTG curves in N_2 atmosphere for the pyrolysis of S, C and T.

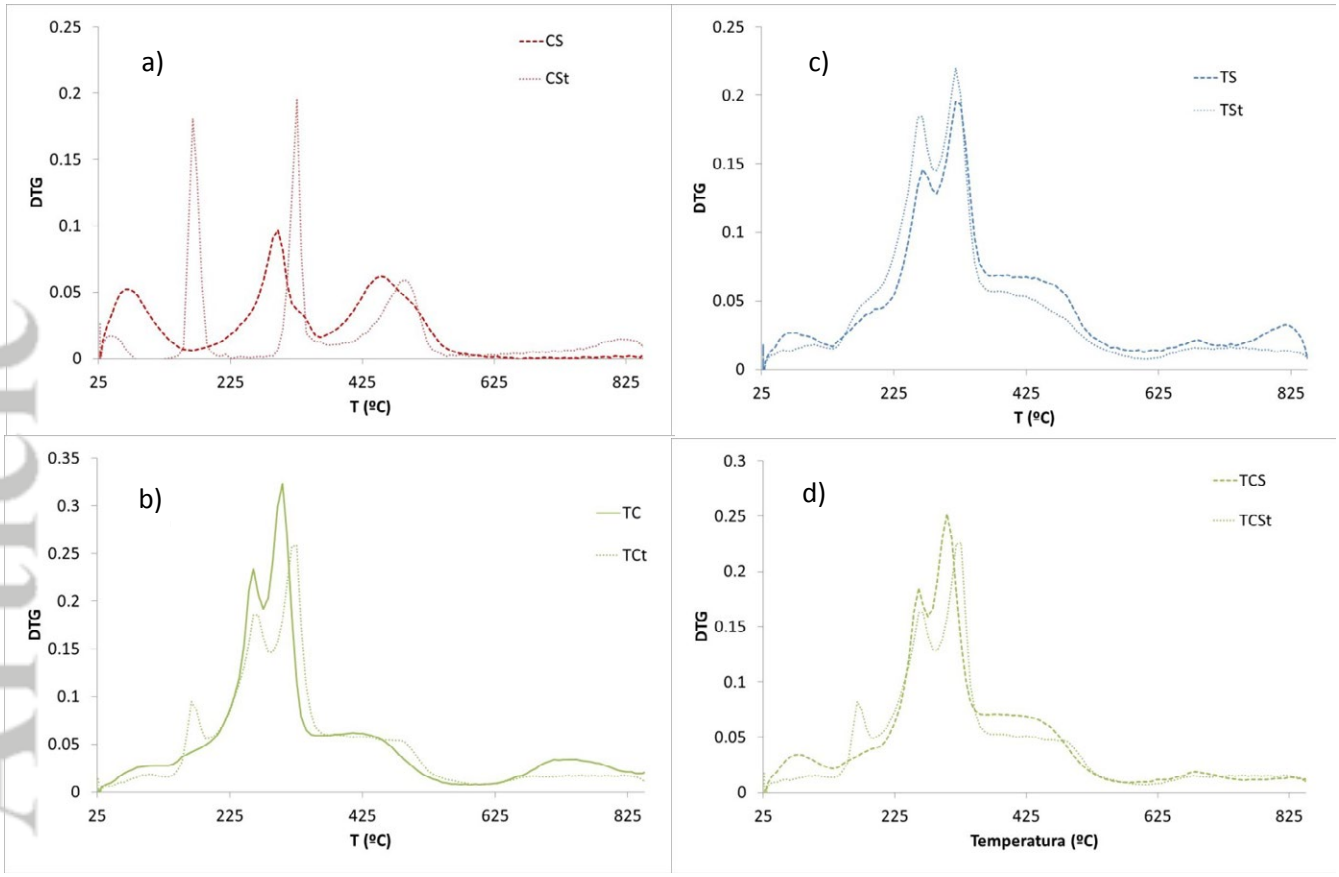

Figure 2. Experimental and theoretical DTG curves corresponding to the pyrolysis of: a) CS, b) TC, c) TS and d) TCS and sample in N_2 atmosphere.

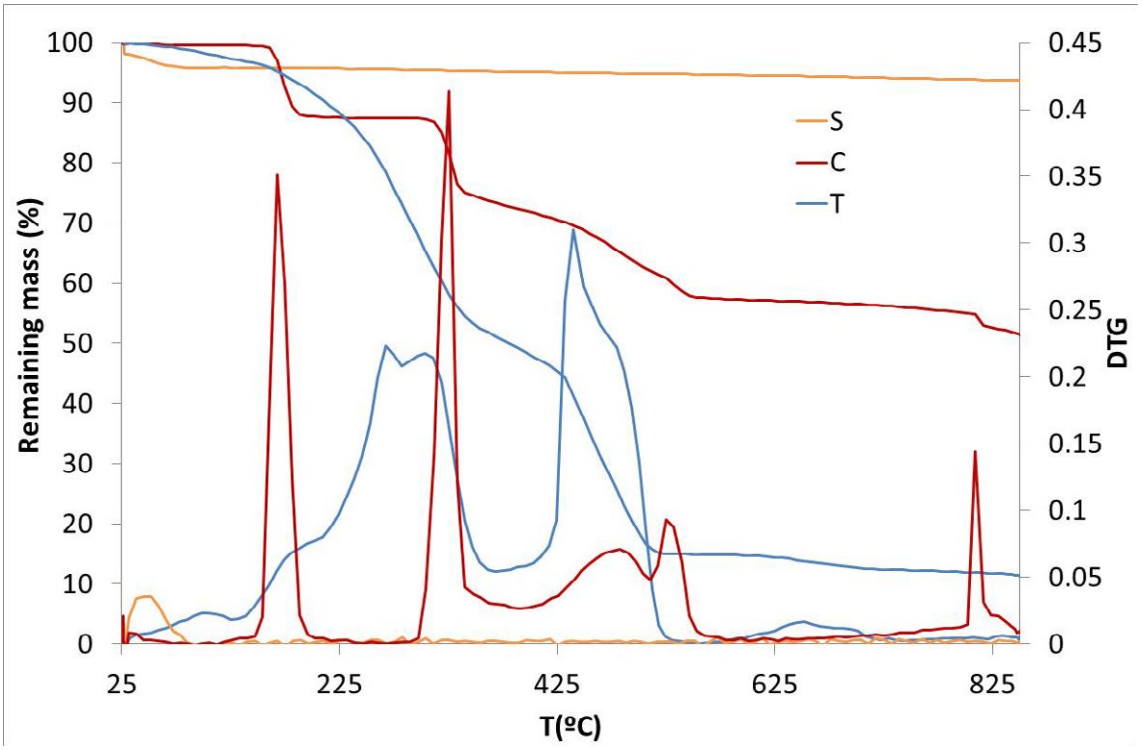

Figure 3. TGA and DTG curves under Air atmosphere for the pyrolysis of S, C and T.

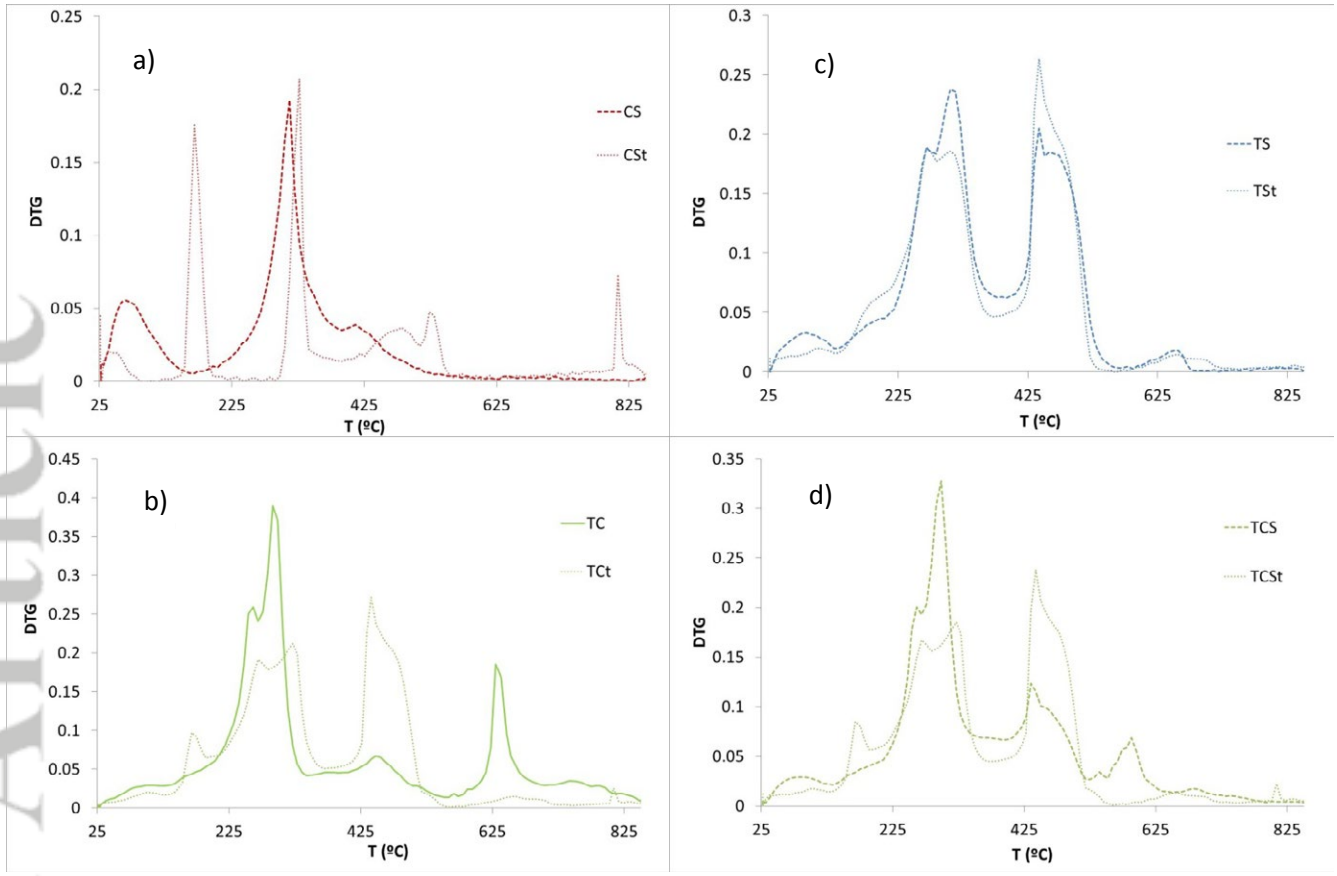

Figure 4. Experimental and theoretical DTG curves corresponding to the pyrolysis of: a) CS, b) TC, c) TS and d) TCS and sample in air atmosphere.

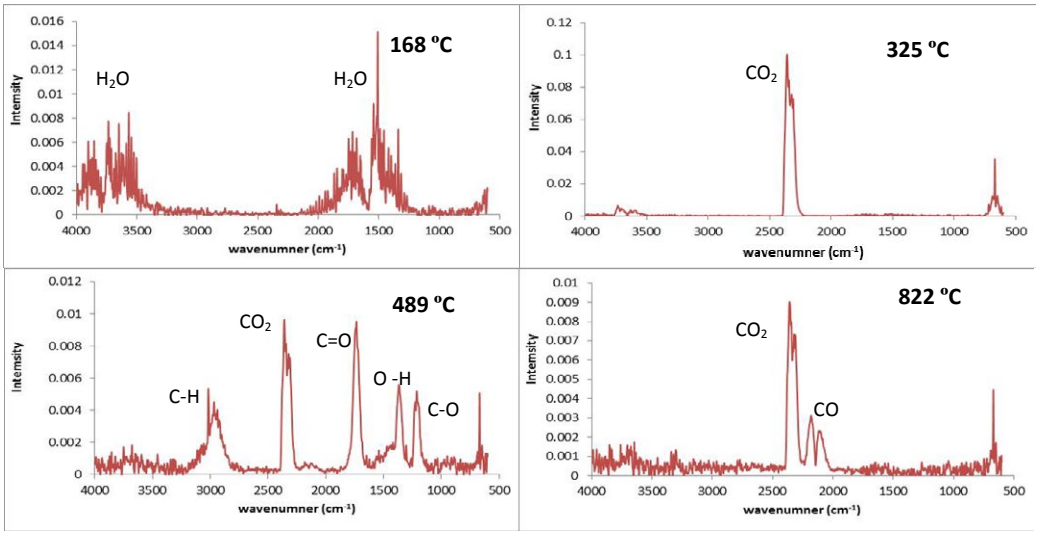

Figure 5. FTIR spectra corresponding to the gas evolved at several selected temperatures in the TGA analysis in N_2 atmosphere of sodium citrate.

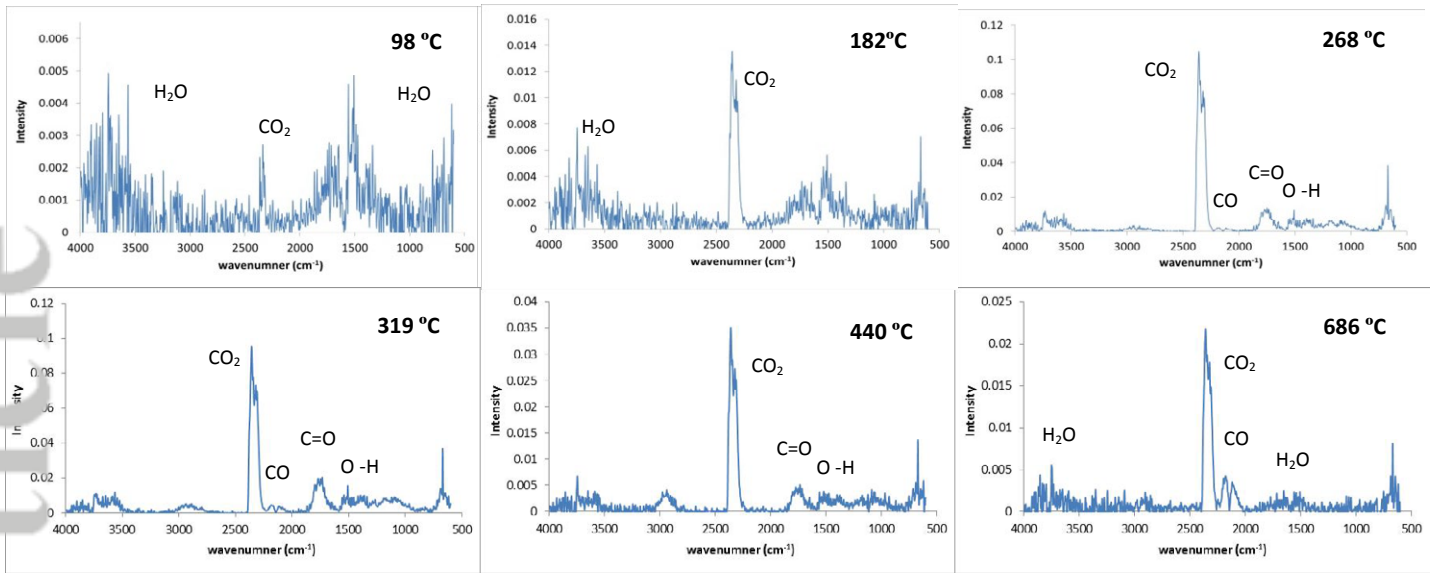

Figure 6. FTIR spectra corresponding to the gas evolved at several selected temperatures in the TGA analysis in N_2 atmosphere of tobacco.

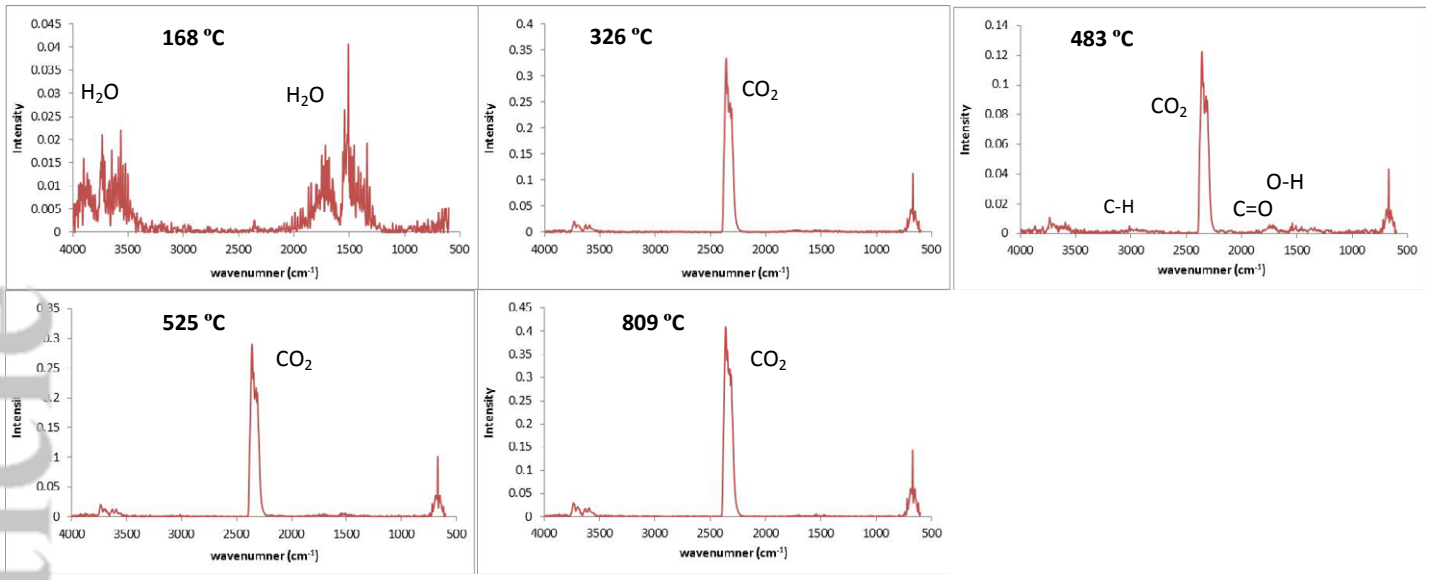

Figure 7. FTIR spectra corresponding to the gas evolved at several selected temperatures in the TGA analysis in air atmosphere of sodium citrate.

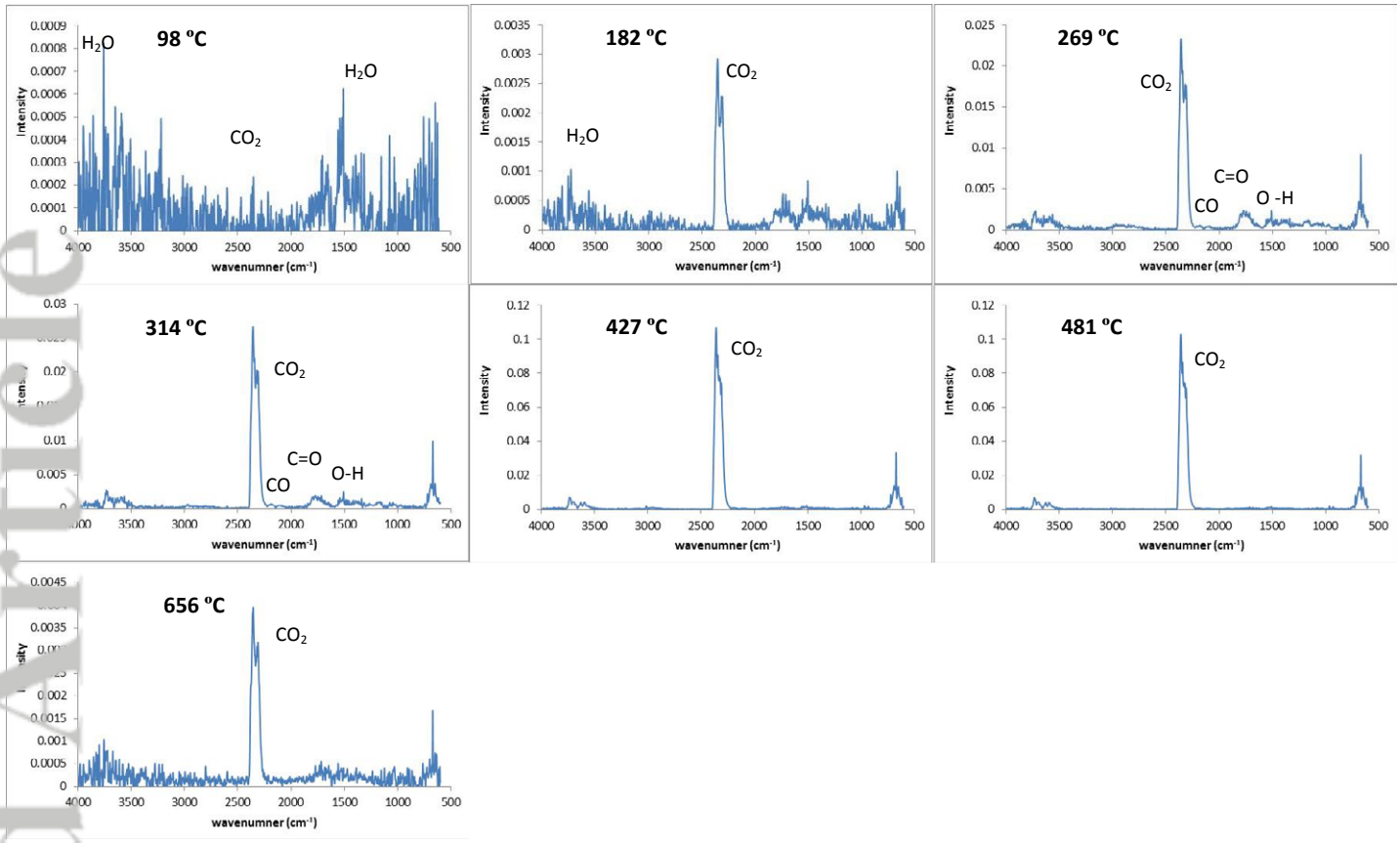

Figure 8. FTIR spectra corresponding to the gas evolved at several selected temperatures in the TGA analysis of tobacco in air atmosphere.

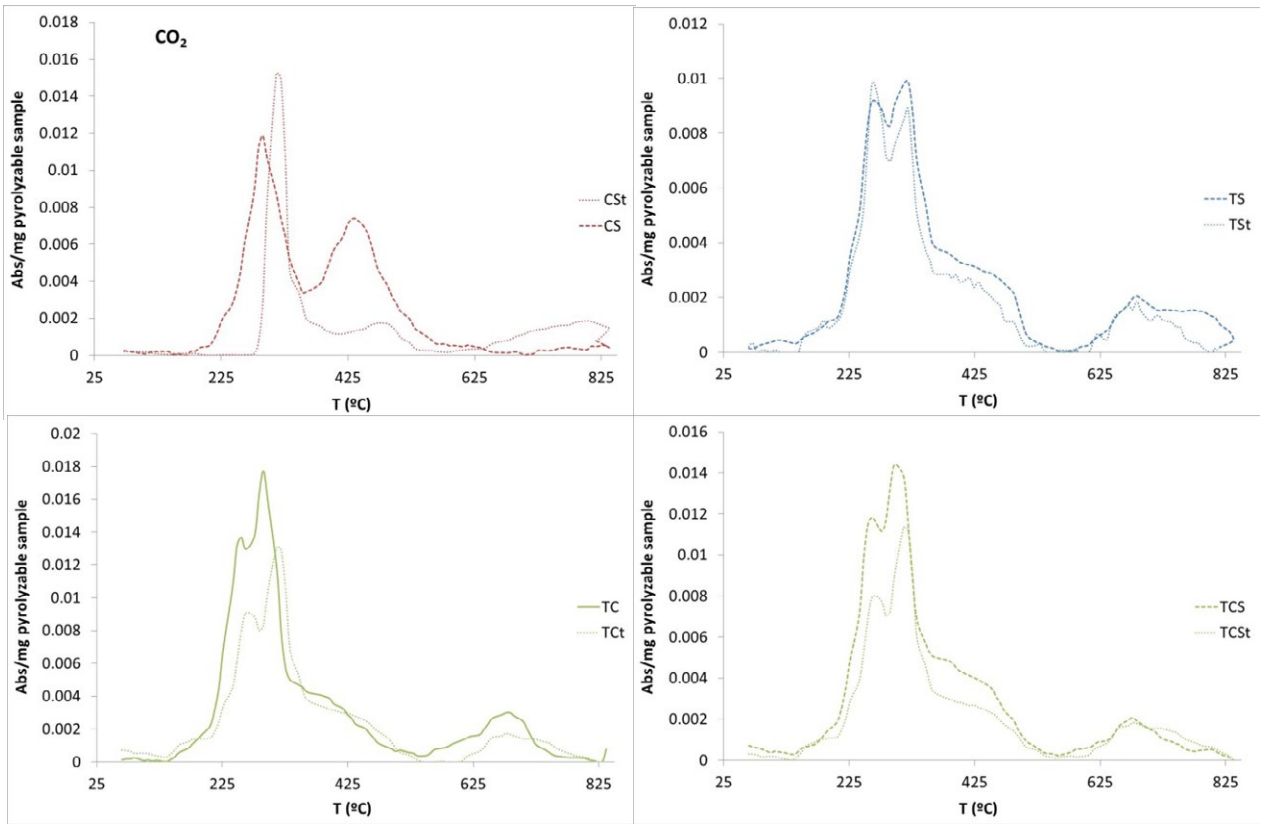

Figure 9a.

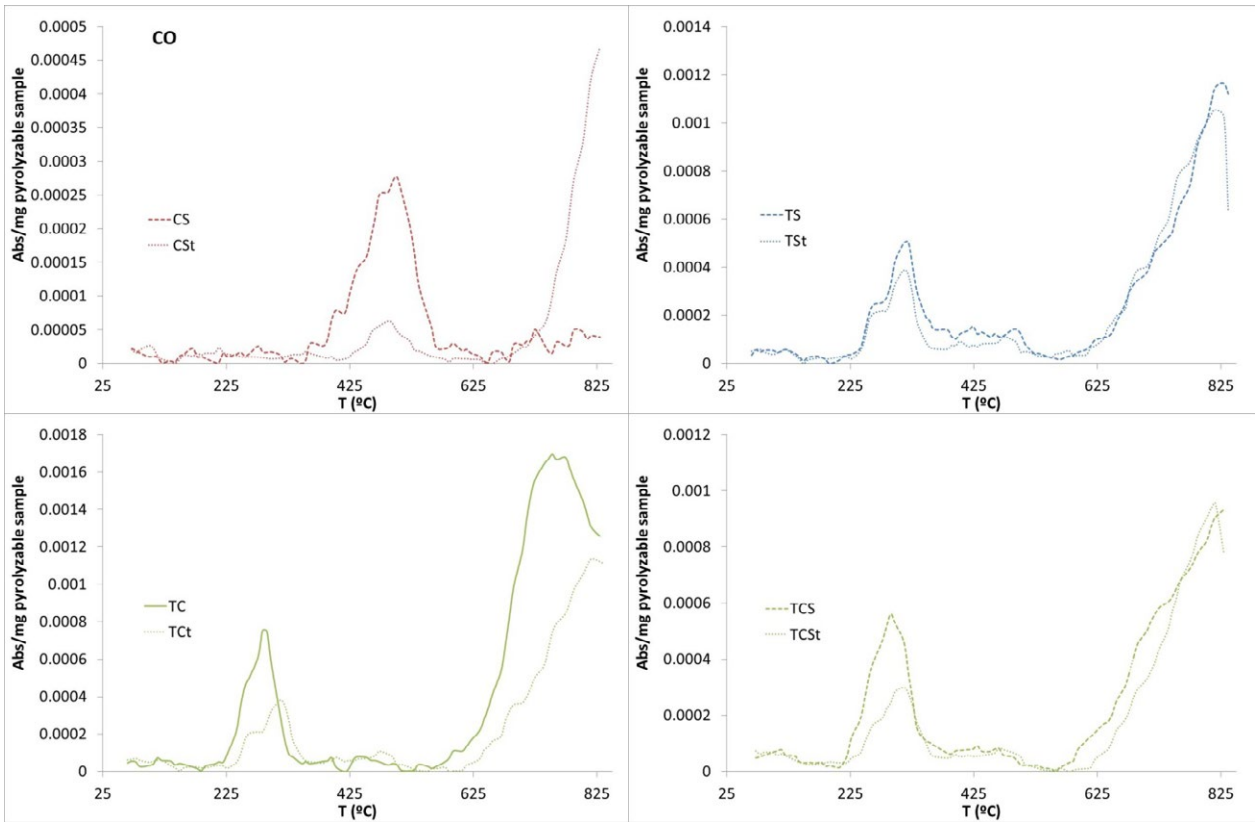

Figure 9b.

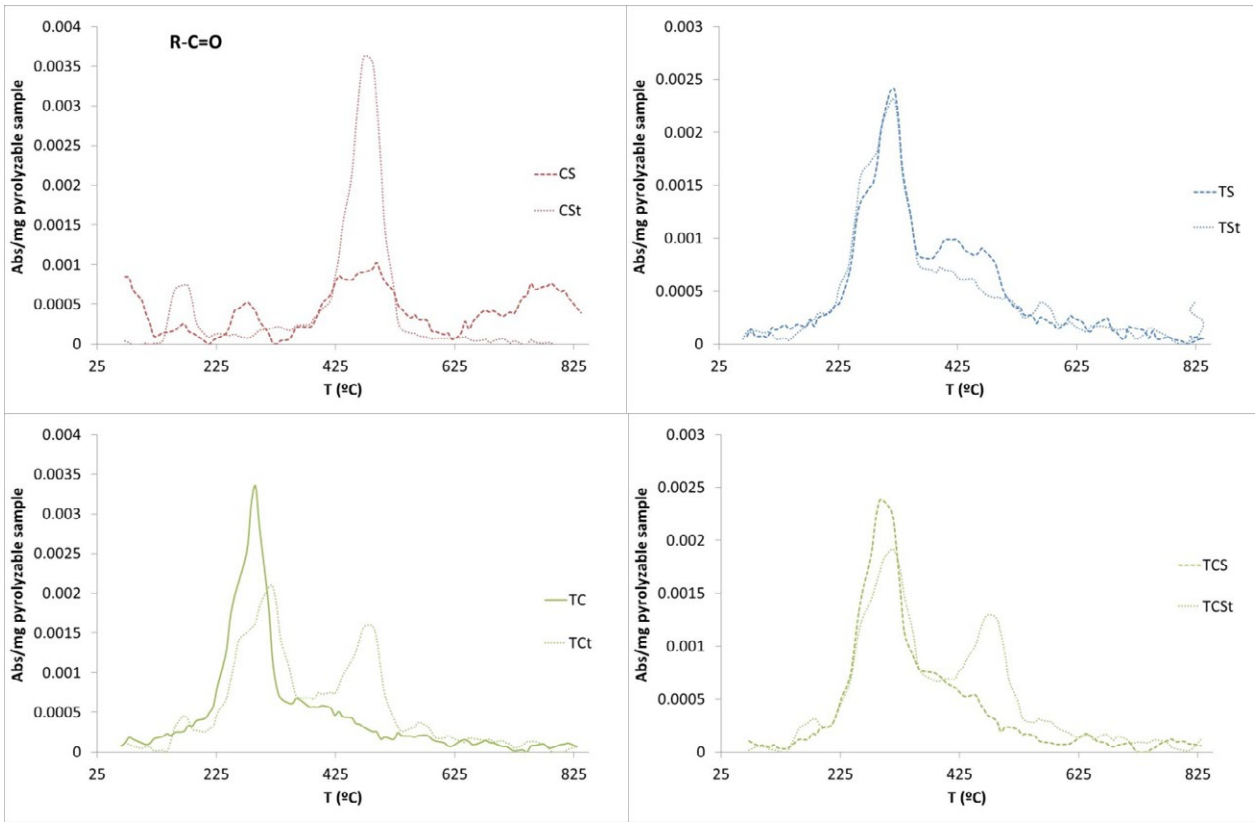

Figure 9c.

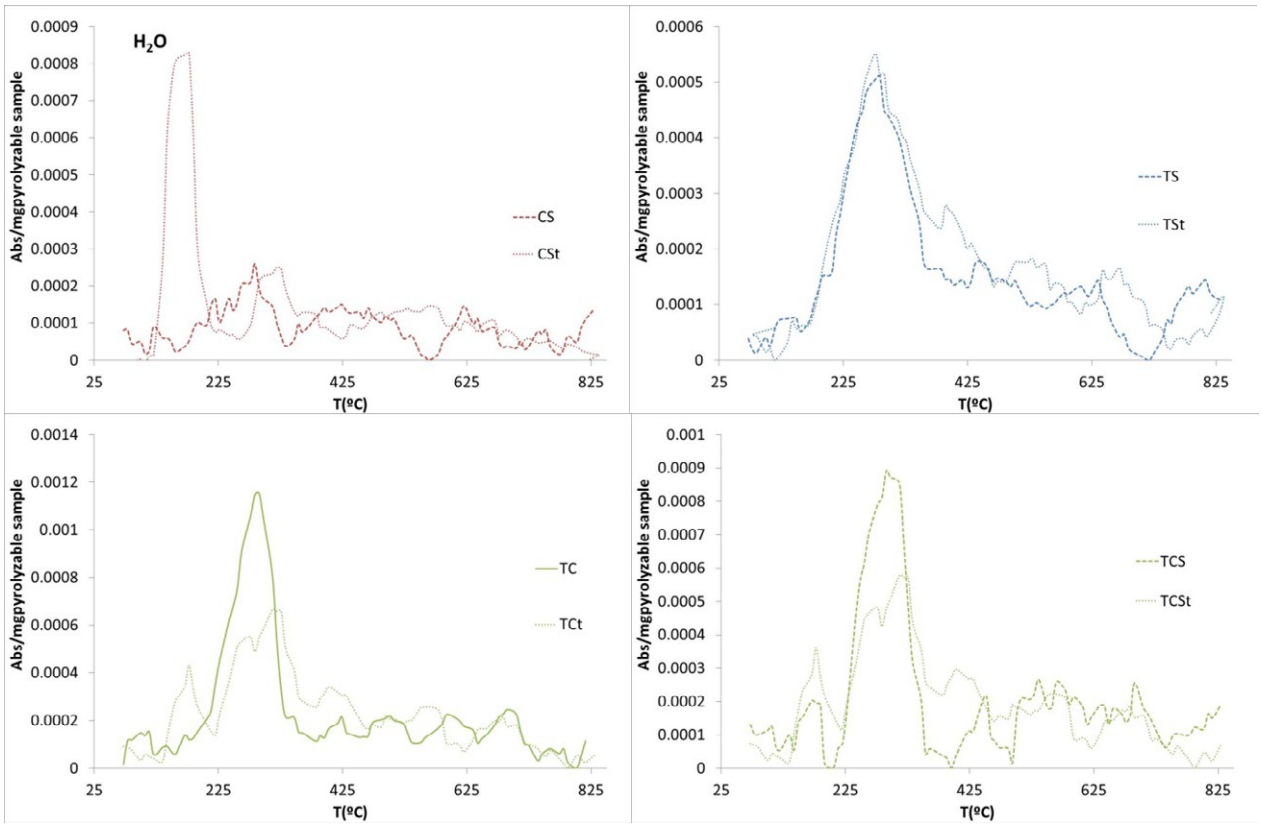

Figure 9d.

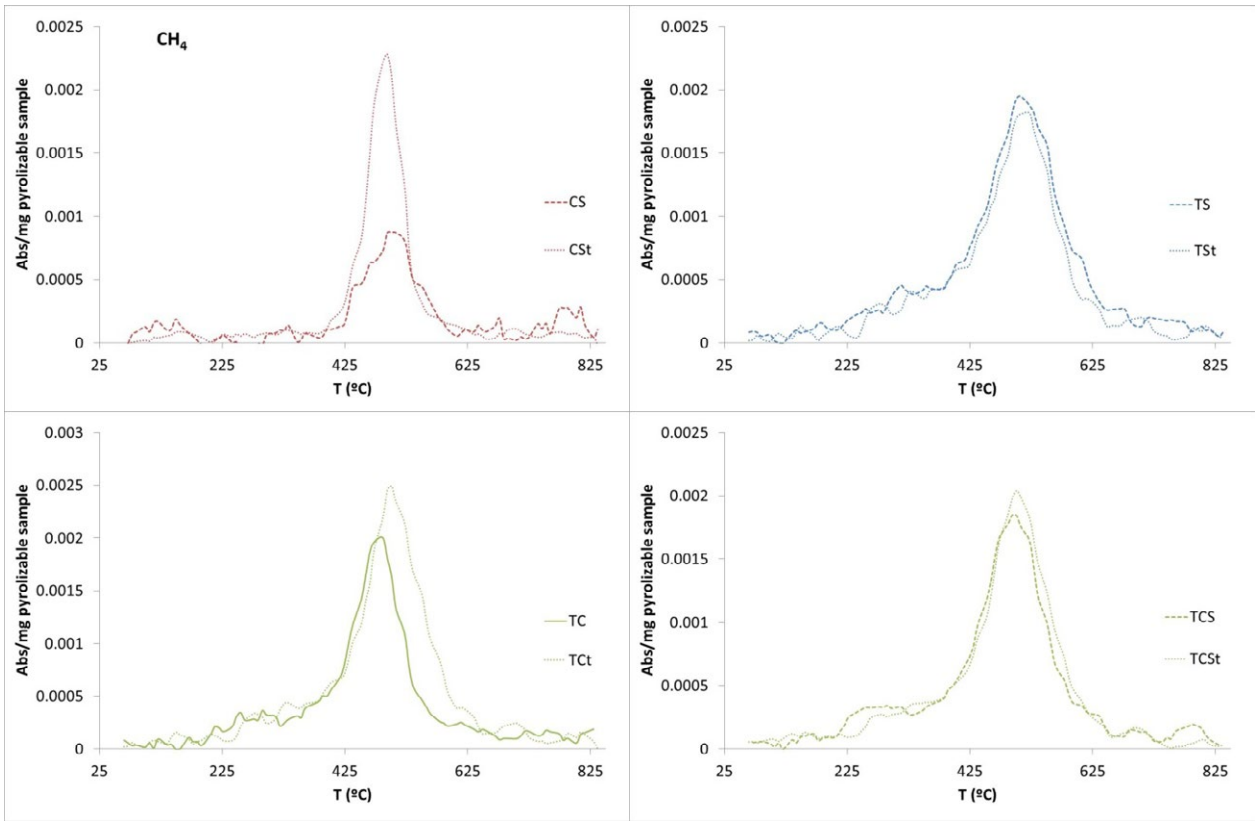

Figure 9e.

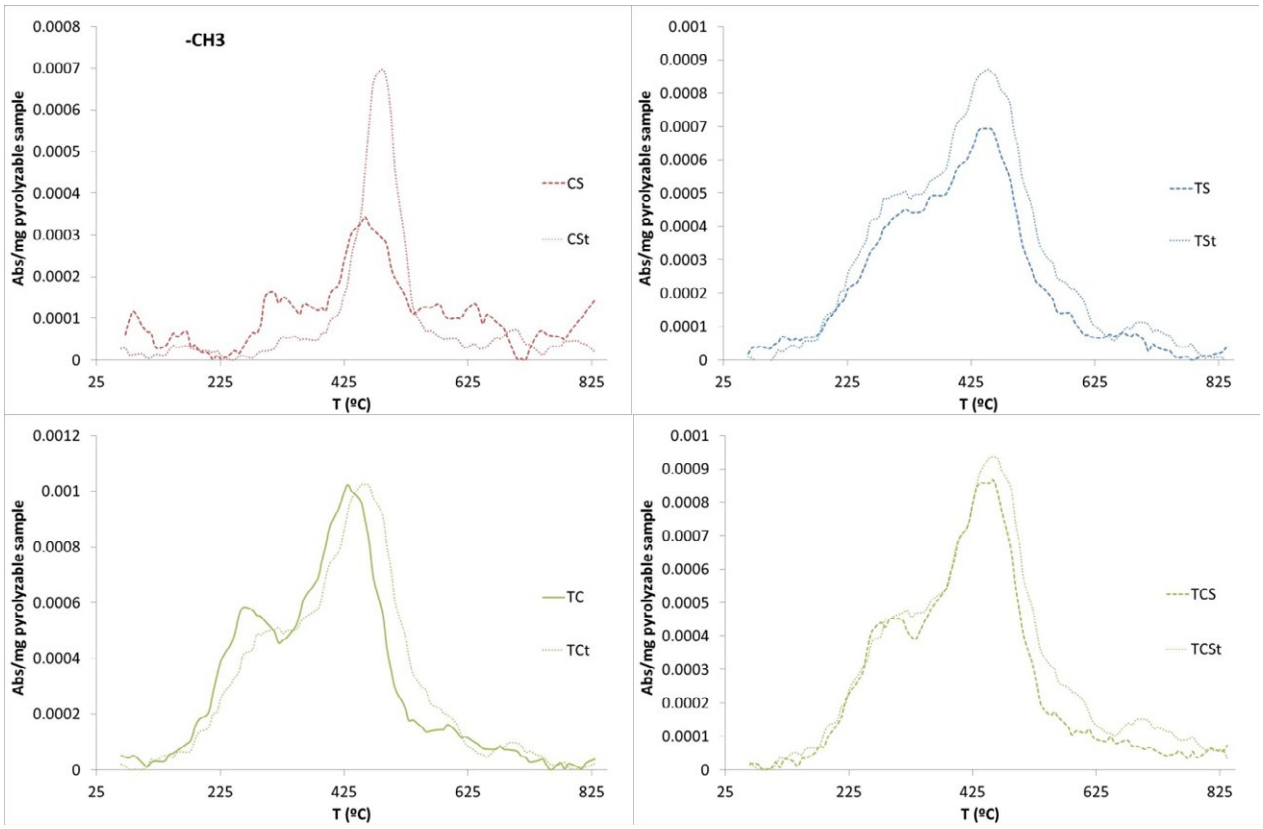

Figure 9f.

Figure 9. Comparison of experimental and theoretical curves of the evolution of the IR bands corresponding to a) CO_2 b) CO, c) carbonyls, d) H_2O, e) $–CH_3$, f) ; in N_2 atmosphere.

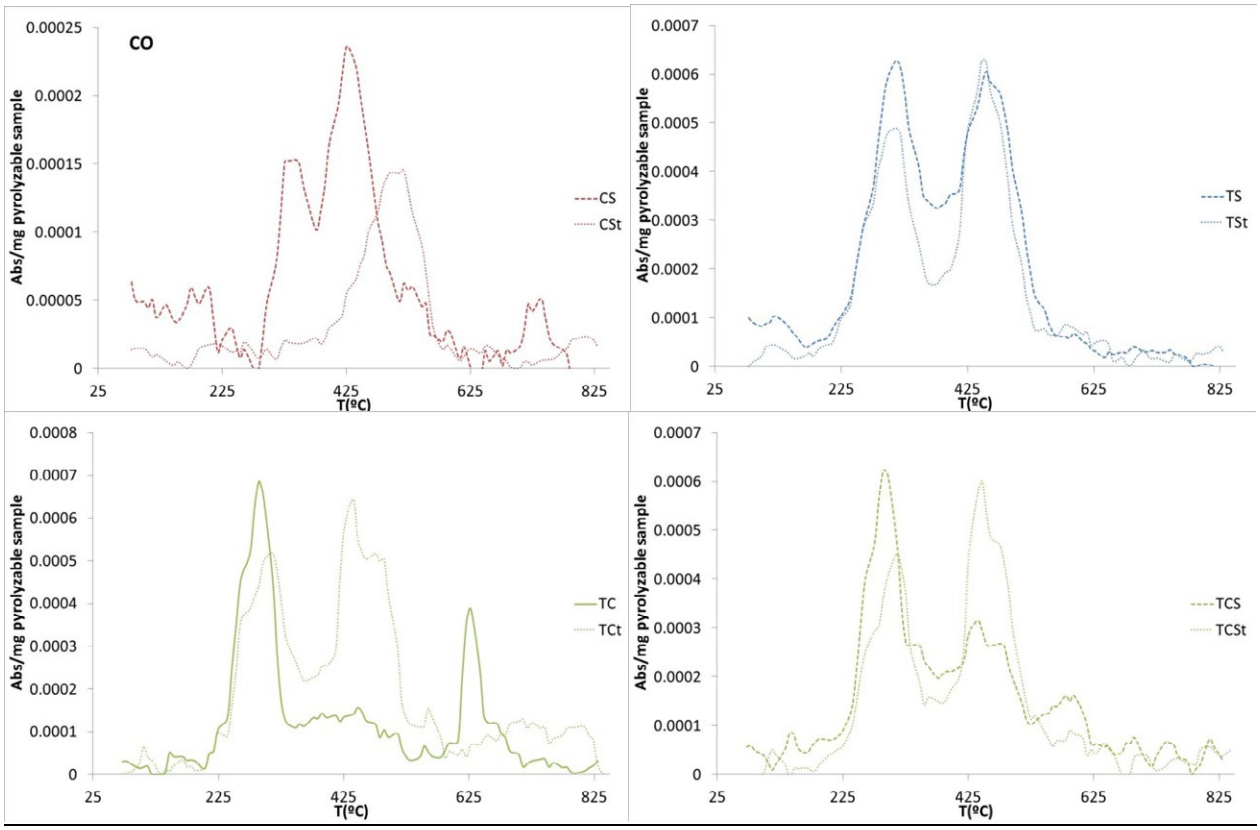

Figure 10a.

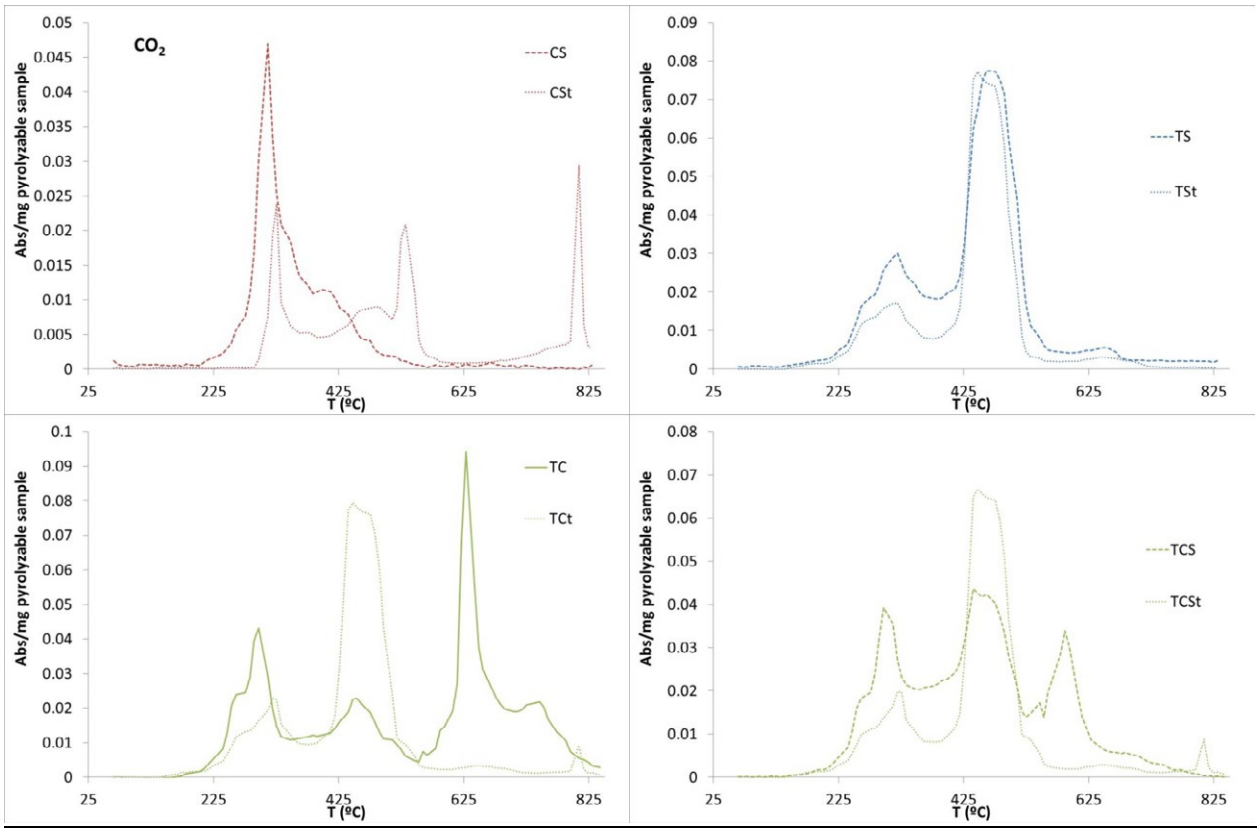

Figure 10b.

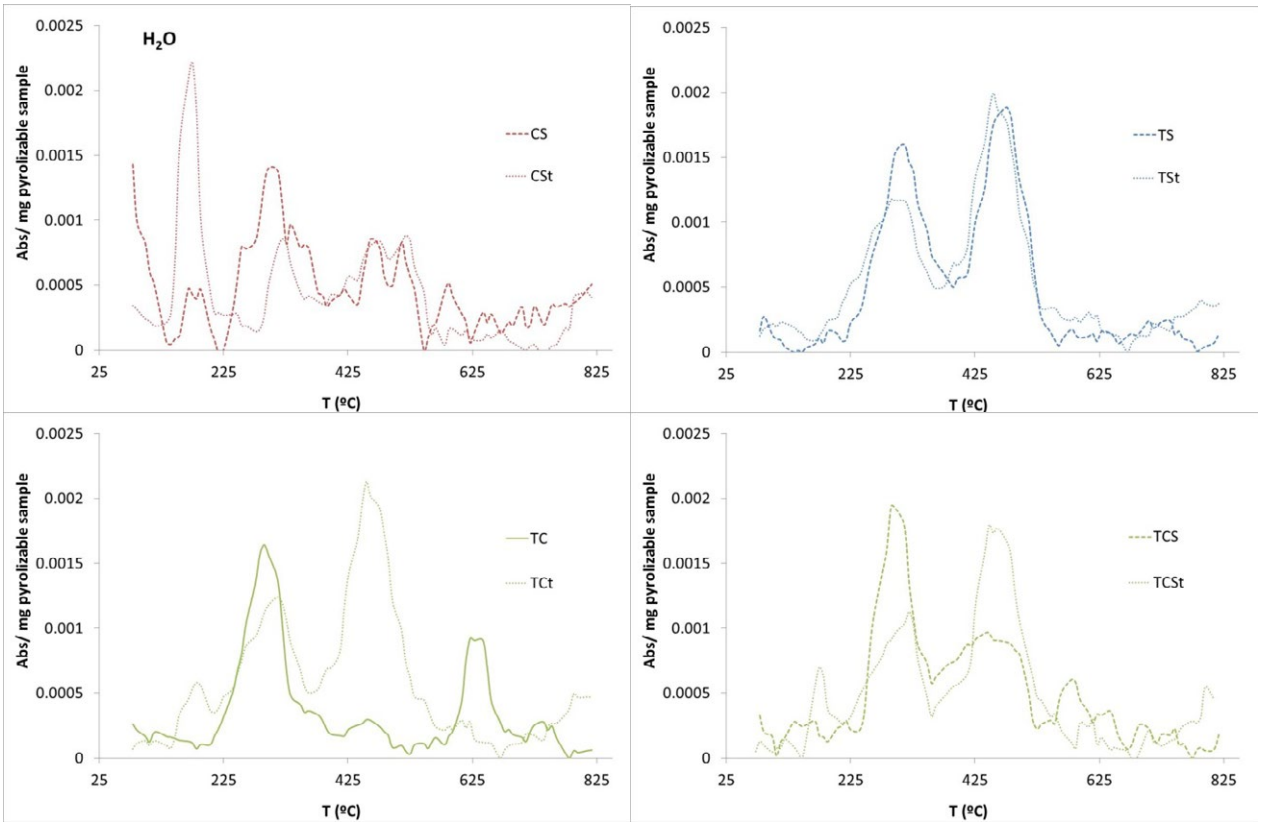

Figure 10c

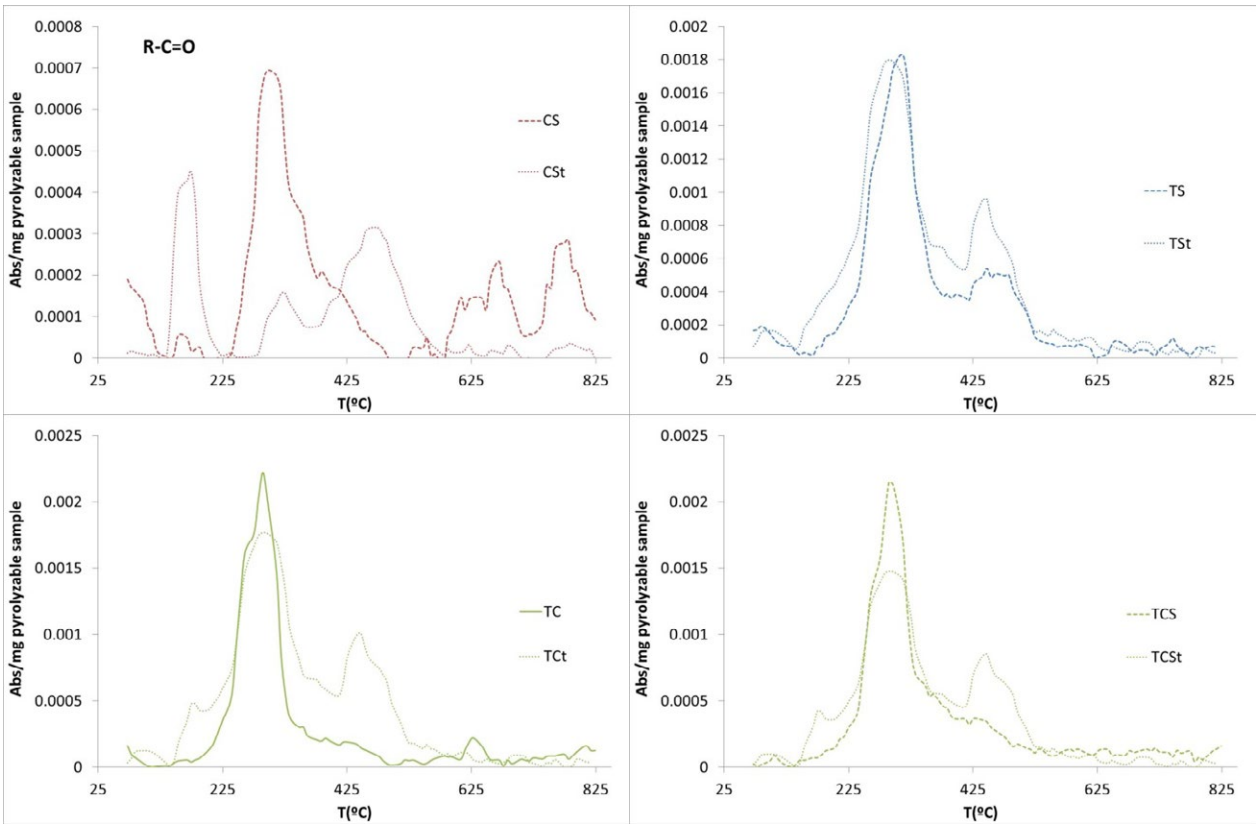

Figure 10 d.

Figure 10. Comparison of experimental and theoretical curves of the evolution with the temperature of the IR bands corresponding to: a) CO_2, b) CO, c) carbonyl and d) H_2O, in air atmosphere